Macromolecules
ARTICLE

Macromolecules **2009**, *42*, 5139–5145 **5139**
DOI: 10.1021/ma900520v

Dimensional Scaling of Cylinders in Thin Films of Block Copolymer−Homopolymer Ternary Blends

Karl O. Stuen,[†] Carla S. Thomas,[†] Guoliang Liu,[†] Nicola Ferrier,[‡] and Paul F. Nealey*,[†]

[†]*Department of Chemical and Biological Engineering and* [‡]*Department of Mechanical Engineering, University of Wisconsin, Madison, Wisconsin 53706*

Received March 10, 2009; Revised Manuscript Received June 1, 2009

ABSTRACT: The cylindrical domain diameter (d), spacing (D), and uniformity in thin films of ternary blends of a cylinder-forming polystyrene-*block*-poly(methyl methacrylate) block copolymer and the corresponding homopolymers were investigated as a function of the molecular weight (M_n) and concentration (φ_H) of the homopolymers. Thin films (20−65 nm) of the blends were deposited on silicon wafers that had been modified with random copolymer brushes such that the cylindrical domains of the annealed blends were oriented perpendicular to the substrate. The best uniformity of d, at a given φ_H, was achieved in the blends with lower homopolymer M_ns. For blends made with homopolymers that had M_n values of the same order of magnitude as those of the corresponding blocks of the copolymer, D increased with increasing φ_H as $D = D_0(1 - \varphi_H)^{-\beta}$, where D_0 is the domain spacing of the block copolymer and β is a parameter that depends on the ratio of the homopolymer and block copolymer molecular weights. The cylindrical domains of the blends could be swollen up to 150% of the original diameter while maintaining hexagonal ordering. For most of the blends on the random copolymer brushes, uniform arrays of perpendicular cylinders were formed most frequently at a film thickness near D_0. A ternary blend with homopolymers with very low M_ns produced markedly different results: D decreased in size with increasing φ_H, measurable up to $\varphi_H = 0.4$, and produced uniform patterns in films with thicknesses ranging from 20 to 37 nm.

Introduction

The assembly of block copolymer domains in thin films has the potential to significantly improve advanced lithographic processes[1] as well as the fabrication of nanostructured templates.[2] In the case of nanolithography, the directed assembly of block copolymer domains can provide enhanced resolution[3,4] and uniformity[5] of patterned features that match essential integrated circuit geometries.[6] Nanoscale arrays of cylinders are important for applications such as high-density bit patterned media.[3,7] In addition to their potential uses in advanced lithography, block copolymer templates could be beneficial in applications such as patterning monolithic materials for chromatographic and catalytic applications,[2] providing ordered reaction sites for nanoparticle generation,[8] hosting photonic crystals, and creating surfaces for controlled cellular response.[9]

For many applications, a specific domain dimension is required. The domain size of a block copolymer depends on the number of repeat units in the block copolymer (N), the characteristic segment length of the polymer chain, and the Flory−Huggins interaction parameter (χ), which is determined by the physical interaction of the blocks.[10] One approach to realizing specific domain dimensions is to synthesize a new block copolymer for each desired size. An alternative approach is to use a blend of a block copolymer with a homopolymer or with another block copolymer to tune the dimensions of the pattern.[11−17] The addition of homopolymer can swell the block copolymer domains in a controlled fashion,[14,18−20] thereby permitting customization of the domain sizes for each specific application without requiring the synthesis of new materials.

Knowledge of the maximum amount of homopolymer that can be added to a ternary blend without disrupting its microphase-separated morphology is necessary to create uniform nanostructures. While the addition of homopolymer can offer a degree of control of the domain size in a thin film of block copolymer, it can also lead to the formation of morphological phases not observed in pure block copolymers.[21] For example, the addition of a sufficiently large amount homopolymer to a block copolymer will result in the formation of either a microemulsion or a macrophase-separated morphology. In the case of microemulsions of ternary blends, the relative amount of each homopolymer, as well as the mole fraction of each block in the block copolymer, can lead to the formation of either bicontinuous or droplet microemulsions.[22−24] Phase transitions of block copolymer blends have been studied in the bulk[20,21,25−33] and in thin films.[32,34−36] An understanding of the phases and phase transitions of thin films of ternary blends, and how they impact dimensional scaling and domain uniformity, is necessary if thin films of ternary blends are to be optimized for use in technological applications.

In this work we investigated the effect of homopolymer molecular weight (M_n) and concentration (φ_H) on the domain size and uniformity in ternary blends composed of cylinder-forming polystyrene-*block*-poly(methyl methacrylate) block copolymer (PS-*b*-PMMA), polystyrene (PS), and poly(methyl methacrylate) (PMMA). We used fast Fourier transforms (FFTs) of scanning electron microscope (SEM) images to classify each blend as forming one of three phases: microphase-separated, nonuniform, and macrophase-separated phases. Characteristics of the nonuniform phase were similar to those of microemulsions in bulk ternary blends. We produced hexagonal arrays of vertically oriented cylinders by annealing thin (≤65 nm) films of the ternary blend on brushes made from a random copolymer of styrene and methyl methacrylate (PS-*r*-PMMA). Of particular interest was determining the homopolymer M_n values that would lead to uniform patterns in thin films of the ternary blends. The center-to-center domain spacing (D), cylindrical domain

*Corresponding author. E-mail: nealey@engr.wisc.edu.

Published on Web 06/25/2009

Table 1. Block Copolymer/Homopolymer Blends[a]

label	PS M_n	PMMA M_n	brush regime
1.5-1.5	1.5	1.5	wet
21-21	21	21	dry
21-37	21	37	dry
39-21	39	21	dry
39-37	39	37	dry

[a]All blends use a 46-*b*-21 PS-*b*-PMMA block copolymer. All molecular weights are in kg/mol.

diameter (d), and the degree of nonperpendicular "defect" structures in the films were analyzed as a function of both film thickness and φ_H for each blend.

Experimental Section

Materials. The block copolymer and homopolymers were purchased from Polymer Source (Dorval, Quebec) and used as received. These included PS-*b*-PMMA (PS 46 kg/mol, PMMA 21 kg/mol, polydispersity index (PDI) = 1.11), PS homopolymers with molecular weights of 1.25, 20.8, and 38.9 kg/mol and PDIs of 1.10, 1.23, and 1.08, respectively, and PMMA homopolymers with molecular weights of 1.5, 21.2, and 37 kg/mol and PDIs of 1.07, 1.15, and 1.04, respectively.

The PS-*r*-PMMA random copolymer was synthesized using nitroxide-mediated living free radical polymerization, yielding PS-*r*-PMMA with a styrene mole fraction of 61%. Styrene and methyl methacrylate were purchased from Aldrich and distilled prior to polymerization. An alkoxyamine-based initiator was synthesized following the general procedures outlined by Benoit et al.[37] The initiator included an end hydroxyl group for bonding to the Si wafer.[38]

Sample Preparation. The block copolymer−homopolymer blends were prepared as 1% or 1.5% w/w solutions in toluene. For each blend, PS and PMMA were added in a ratio of ~70:30 to the PS-*b*-PMMA to preserve the overall volume fraction of PS and PMMA in the blend. The various blends are listed in Table 1. The brush regime designation is explained in the Discussion section.

The PS-*r*-PMMA was covalently grafted to the native oxide on silicon wafers, as described previously.[39] Si wafers were cleaned with piranha solution (*caution!*), rinsed with DI water, and dried with a stream of N_2. They were then immediately spin-coated with a 1.5 wt % solution of PS-*r*-PMMA in toluene. The wafers were then annealed at 160 °C under vacuum for 48 h to graft the PS-*r*-PMMA to the substrate through a dehydration reaction. Ungrafted PS-*r*-PMMA was removed via repeated sonication in warm toluene, and the substrates were dried under nitrogen. The block copolymer blends were then spin-coated onto the brushes over a range of spin speeds to achieve the desired film thickness. Blends 21-21, 21-37, 39-21, and 39-37 (referred to throughout as the dry brush blends) were coated to yield films with thicknesses ranging from 33 to 65 nm. Blend 1.5-1.5 (referred to as the wet brush blend) was coated to produce films 20 to 38 nm thick. These thicknesses were chosen to be near D for the various blends. The blend films were annealed at 190 °C for 3 days in a vacuum chamber at ~200 Pa absolute pressure. At this annealing temperature χN of the pure block copolymer was 24.[40] Prior to annealing, the chamber was backfilled with Ar.

For pattern transfer to the silicon wafer, the PMMA was first removed with a wet etch process. For the wet etching, the block copolymer film was irradiated with UV light with a maximum intensity at 254 nm with an exposure of 0.45 J/cm^2. The samples were then dipped in glacial acetic acid for 1 min, soaked in deionized water for 1 min, and dried over N_2. Finally, the nanoporous templates were dry etched to transfer the pattern into Si. A helicon plasma source was used with Ar, SF_6, and $C_2H_2F_4$ gases at flow rates of 60, 9, and 9 sccm, respectively. The etching was performed at 1.3 Pa and at a wafer temperature of 5 °C. A source power of 600 W was used with a −80 V wafer bias voltage. Approximately 60% of the PS template was removed during the dry etch process. The remaining PS template was removed using an oxygen plasma (5 min, unbiased chamber under vacuum to 9.3 Pa, oxygen flow rate of 50 sccm, applied power of 250 W at 13.56 MHz).

Materials Analysis. A ^{1}H NMR spectrum was recorded for the PS-*r*-PMMA in solution ($CDCl_3$) with a Bruker AC+ 300 (300-MHz) spectrometer. GPC was performed on the homopolymers with a Viscotek GPCmax instrument with two columns (Varian 5M-POLY-008-27 and 5M-POLY-008-32) and model 302 TDA detectors. The polymers were eluted with THF at a flow rate of 1 mL/min at 30 °C. PS M_n and PDI values and PMMA PDI values were determined using a refractive index detector and calculated as PS equivalents. The PMMA M_n values listed were those quoted by Polymer Source. The film thicknesses of the brush and block copolymer layers were measured with a Rudolph Research Auto EL ellipsometer. Top-down SEM images of the block copolymer microdomains and Si structures were acquired with a LEO-1550 VP field-emission instrument using an accelerating voltage of 1 kV and a 30 μm aperture.

To determine d, we used custom software employing a gradient technique, which evaluates the brightness near the block copolymer interface in an SEM image and marks the steepest slope as the domain edge. Azimuthally averaged FFTs of the SEM images were used to determine domain spacings ($D = (2/\sqrt{3})(2\pi/q)$, where q is the location of the first-order peak) and phase transitions. The disappearance of the second- and first-order peaks in the FFTs as φ_H was increased from $\varphi_H = 0$ was used to demarcate the microphase-separated, nonuniform, and macrophase-separated phases.

Results

After annealing on the random copolymer brush, the blend films contained PMMA cylinders that were oriented perpendicular to the substrate, as shown in the SEM images of blend 21-21 in Figure 1. Figure 1 (left) shows top-down SEM images of the free surface of films of blend 21-21 (thickness 30−60 nm) for a range of φ_H values. At low φ_H values ($\leq$0.2), the cylindrical domains were small and uniform. As φ_H increased, the size and spacing of the cylinders increased, as can be seen visually by comparing the images at $\varphi_H = 0$ and $\varphi_H = 0.4$. Some deformed cylinders were present, but in general the cylinders remained in a hexagonal arrangement. As φ_H was increased further to 0.5 and larger values, the cylinders became very nonuniform in size and shape. In contrast, for blend 1.5-1.5, the size of the domains and sharpness of the interfaces decreased as φ_H was increased from $\varphi_H = 0$.

For all φ_H values of blend 21-21, the cylinders penetrated through the entire thickness of the film, as evidenced by the pores that could be made in the underlying silicon by using the blend film as an etch mask (see Supporting Information). The uniformity and dimensions of the etched pore structures varied with φ_H in the same way as the cylinders in the blend film, indicating that the spot structures seen in the SEM images of the blend film were cylinders that spanned the thickness of the film.

The domain spacing D as a function of φ_H was characterized for each of the blends, as shown in Figure 2. D was calculated from the peak position of an azimuthally averaged FFT of a top-down SEM image of the blend. All of the blends followed the same general trend of D increasing with φ_H, except for blend 1.5-1.5. Blend 1.5-1.5 followed a different trend, with the domain spacing slightly decreasing with increasing φ_H. The spacings from films of blend 1.5-1.5 with $\varphi_H > 0.4$ were not determined because of the diminishing contrast between PS and PMMA when $\varphi_H >$ 0.4 and the concomitant difficulty in extracting the domain

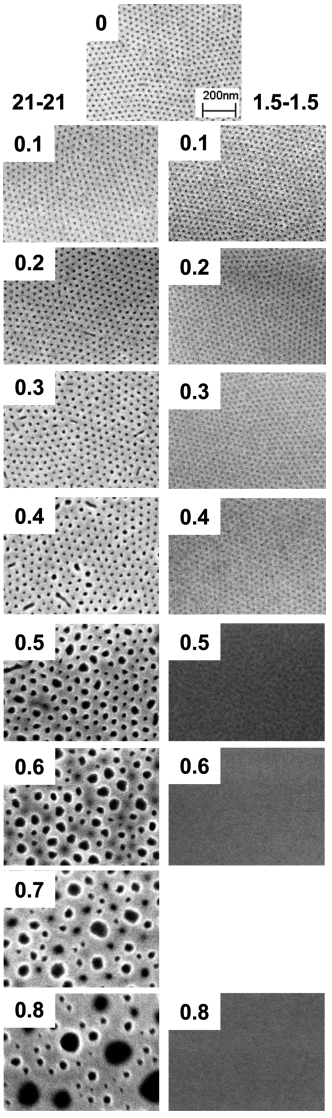

Figure 1. Top-down SEM images of the 21-21 blend (left) and the 1.5-1.5 blend (right). The volume fraction of homopolymer added is shown in the upper left corner of each image. The scale bar applies to all images.

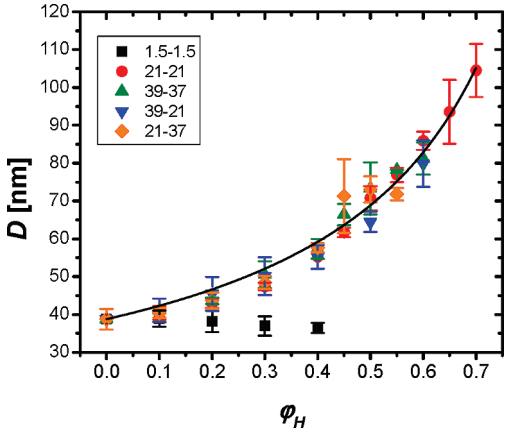

Figure 2. D (center-to-center cylinder spacing) as a function of φ_H for the different blends. The black line is a plot of eq 1 with $\beta = 0.83$.

spacing. All of the 1.5-1.5 films yielded excellent perpendicular orientation and hexagonal ordering and showed few, if any, defects. Throughout this study, the term "defect" refers to any structure other than circular spots (as seen from the top-down SEM) formed from the perpendicular cylinders. Parallel, twisted or angled cylinders, and loop structures are all classified as defects.

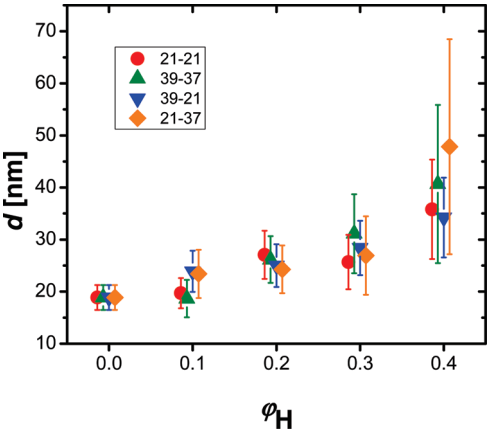

Figure 3. Spot diameter, d, as a function of φ_H for the different blends. The error bars represent one sigma.

The size and variation of d also increased with increasing φ_H, as shown in Figure 3. The values of d and the corresponding standard deviations were calculated for the dry brush blends with $0 \leq \varphi_H \leq 0.4$. As shown in Figure 3, the variation in d increased in the following order: 39-21, 21-21, 39-37, 21-37. The standard deviation of d increased more rapidly for the blends with higher PMMA M_n. Similarly, at the highest φ_H in the range in Figure 3 ($\varphi_H = 0.4$), d was larger when the PMMA M_n was larger (blends 39-37 and 21-37).

Along with φ_H, film thickness also had an effect on nanopattern quality and uniformity. Figure 4 shows the pattern quality as a function of the combined effects of D, φ_H, thickness, and blend. In the graph of D versus film thicknesses (Figure 4), blend compositions are denoted by the different shapes of the data points. The dashed lines parallel to the x-axis demarcate regions of constant φ_H. The quality of the pattern of perpendicular cylinders of each blend was visually assessed and categorized as having poor, medium, or high quality. Representative SEM images of each quality classification are shown on the right side of Figure 4. The size of each data point reflects the quality observed in each self-assembled blend (smaller points = higher quality). The pure block copolymer produced good quality perpendicular structures over a wide range of thicknesses. As φ_H was increased in the blends, more defects were observable in the annealed films and the range of thicknesses that yielded quality films decreased. The best quality films were found most frequently near a thickness of 38 nm, regardless of φ_H. For those films with large φ_H ($\varphi_H = 0.3$) and therefore large D, increasing the film thickness to approximately match D did not increase the pattern quality. In contrast to the results shown in Figure 4, blend 1.5-1.5 (not shown) produced perpendicular structures without defects over a range of thicknesses and φ_H values.

The disappearance of the first- and second-order peaks in the FFTs as φ_H was increased from 0 to 0.8 was used to determine phase transitions in the blends, as shown in Figure 5. In both blend samples presented in Figure 5, the second-order ($\sqrt{3}$) peak disappeared between $\varphi_H = 0.5$ and 0.6. In previous studies the disappearance of the higher-ordered peak in small-angle neutron scattering (SANS) profiles of ternary blends was used to indicate the transition from a microphase-separated phase to a microemulsion phase.[21,22] Here we viewed the disappearance of the $\sqrt{3}$ peak as indicative of the transition from the ordered, microphase-separated phase to the nonuniform phase. The transition from the nonuniform phase to the macrophase-separated phase was apparent in the disappearance of the first-order peak between

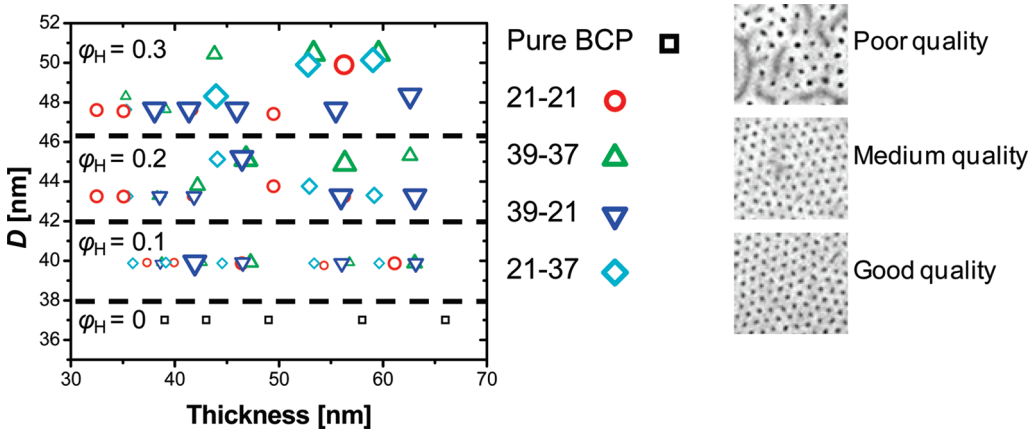

Figure 4. Quality of perpendicular cylinders as a function of film thickness, domain spacing, and blend. The size of each point is relative to the observed quality of each image (small = good quality, large = poor quality). SEM images are representative of quality categories. The dashed lines separate data based on the amount of homopolymer added, and φ_H is given for each region.

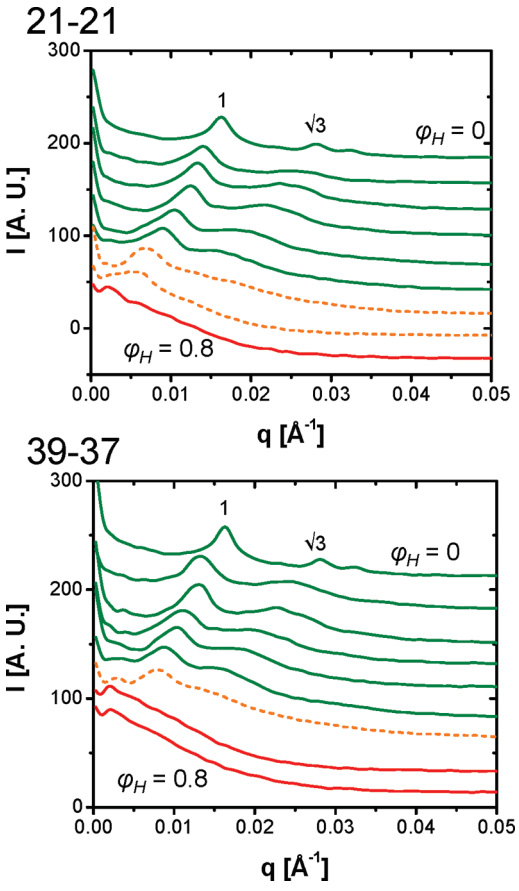

Figure 5. Azimuthally averaged FFTs as a function of blend composition. The curves are offset by an arbitrary amount for clarity. From top to bottom the plots correspond to $\varphi_H = 0$ to 0.8 in 0.1 increments. Solid green lines indicate the microphase-separated phase, dashed orange lines indicate the nonuniform phase, and solid red lines indicate the macrophase-separated phase, as determined by the existence of the first- and second-order peaks for each value of φ_H.

$\varphi_H = 0.6$ and 0.8 for the dry brush blends. In general, the FFTs of the SEM images of the dry brush blends were similar. For the wet brush blend (blend 1.5-1.5, not shown) the FFT did not show sharp peaks because of the poor contrast between the domains and the lack of sharp domain interfaces in the SEM images. The poor contrast and apparent width of the domain interface observed in the SEM images of blend 1.5-1.5 increased with increasing φ_H.

Discussion

Effect of Blend Composition on Domain Spacing and Spot Size. The dry brush blends all showed similar trends of D increasing with φ_H. The relationship between D and φ_H shown in Figure 2 suggests that if a certain spacing were desired, it could be produced by adding the corresponding amount of homopolymer. Using the following empirical relationship, we fit an equation for D as a function of φ_H:[34]

$$D = \frac{D_0}{(1-\varphi_H)^{\beta}} \quad (1)$$

where D_0 is the center-to-center domain spacing of the pure PS-*b*-PMMA. The best fit of the dry blends to this equation yielded $\beta = 0.83$, as plotted in Figure 2. The value of $\beta = 0.83$ was between the experimentally determined β values for lamellar blends reported by Stoykovich et al.[35] ($\beta = 0.74$) and Liu et al.[34] ($\beta = 0.91$) and agreed with the model proposed by Torikai et al.,[14] for a block copolymer blended with homopolymers that had M_n values equal to ~40% of the total block copolymer M_n. The experimental work of Stoykovich et al., Liu et al., and Torikai et al. was for lamellae-forming blends, and it was interesting that β was similar for the lamellae- and cylinder-forming block copolymer blends where the homopolymer/block copolymer M_n ratio was similar.

Considering the images in Figure 1, the hexagonal ordering of the structure only remained up until about $\varphi_H = 0.4$. Beyond this value of φ_H, not only did the hexagonal lattice of spot centers break down, with the spots randomly positioned, but also d varied significantly. Within the range $0 \le \varphi_H \le 0.4$, where better hexagonal ordering and low d variation were achieved, it was still possible to increase d and D up to about 150% of the original size.

The dry brush blends showed differences in the variation in d at $\varphi_H = 0.3$ and 0.4 that depended on the M_n of the PMMA. The variation in d increased more when the M_n of the minority component (PMMA) in the blend was larger. It is interesting to note that the blends with PMMA homopolymer with approximately the same M_n as the PMMA block of the PS-*b*-PMMA had less variation in d than the blends with higher M_n PMMA. The blends with the higher M_n PMMA in the cylindrical domains (39-37 and 21-37) may have produced more variation in d because of a decreased ability, when compared to blends containing the lower M_n PMMA, to achieve equilibrium under our annealing conditions. For equilibrium to occur in a thin film of

perpendicular cylinders, the PMMA chains must diffuse from one cylinder through the PS matrix to the next PMMA cylinder until they are evenly distributed. There is a free energy barrier, however, for a PMMA chain to cross through the PS matrix of the pattern. For the higher M_n PMMA homopolymers, this penalty is larger because more PS−PMMA contacts are formed as the homopolymer passes through the matrix. The large free energy barrier for high M_n PMMA to diffuse may prevent the diffusion of the PMMA homopolymer and cause the system to become trapped in a metastable state with cylinders of various sizes. This mechanism leading to a large spot size variation would be unique to the perpendicular cylinder structure and other structures with isolated domains (such as spheres) and would not necessarily be seen with parallel cylinders or lamellae where the homopolymer can redistribute along domains without having to cross through the other block.[41] Additionally, the higher M_n homopolymer will inherently diffuse more slowly due to the length of the polymer chain.[42] As a result of the greater free energy barrier and the slower diffusion, the blend system may not reach equilibrium under our experimental conditions, resulting in the d variations seen in the blends with large amounts of high M_n PMMA.

Effect of Film Thickness on Pattern Quality. Film thickness was studied to determine its effect on cylinder quality. From Figure 4 it is clear that as D (or φ_H) increased for the dry brush blends, the range of thicknesses that frequently produced good quality structures decreased. The decreased range of thicknesses was related to the fact that at the highest φ_H values in Figure 4 ($\varphi_H = 0.3$) the pattern quality was frequently poor. The poor pattern quality at $\varphi_H = 0.3$, compared to blends with lower φ_H, may suggest that the free energy minima associated with an ordered, uniform, perpendicular cylindrical morphology in these blends was not deep enough to suppress the formation and persistence of defect structures.[43] As a result, the films with higher φ_H ($\varphi_H = 0.3-0.5$) as well as the thicker films had defect structures such as loops or parallel cylinders, which have been observed previously in cylinder-forming diblock copolymers that were directed to assemble on spotted chemical patterns.[43,44] In contrast, the pure block copolymer films produced good quality structures over a range of thicknesses. In general, for all the dry brush blends the best structures were formed most frequently at a thickness of ~38 nm, which matched what has been reported previously as the best thickness for films of PS-*b*-PMMA with 46 and 21 kg/mol M_n blocks, respectively.[45]

Blend 1.5-1.5 produced excellent patterns over $0 < \varphi_H < 0.4$ and over a range of thicknesses. The addition of the low M_n homopolymer appeared to improve perpendicular ordering and reduce defects. The mechanism that caused this is not well-understood but may involve the plasticization of the block copolymer to improve equilibrium kinetics[32] or the reduction of free energy of the perpendicular structures,[46] thereby increasing the driving force for defect-free ordering. In addition, the low M_n homopolymers may diffuse through the cylinders during annealing to reach the free surface or interface more easily than their higher M_n analogues, and this may add a kinetic effect or equilibrium energy that favors the perpendicular orientation.[47]

Phase Transitions. To understand how much homopolymer can be added to blends without breaking down the local ordering in the thin films, it is important to consider the phase transitions of the blend. As the amount of homopolymer added to the blend was increased, the dry brush blend films transitioned from microphase-separated cylinders to a nonuniform phase and then to macrophase-separated structures,[21,23,25,35,48−55] In general, these phase transitions could be determined by either the shape of the FFT curves or by plotting the amphiphilicity factor[56] (a measure of the block copolymer's ability to compatibilize the homopolymers in a ternary blend[57]) as a function of φ_H. In this work, analyzing the disappearance of the first- and second-order peaks in the FFT plots (Figure 5) gave a clearer indication of the phase transitions in the dry brush blends than plotting the amphiphilicty factor. For the wet brush blend (1.5−1.5, not shown), the transition to a nonuniform phase appeared to occur at much lower values of φ_H ($\varphi_H \sim 0.2$) than for the dry brush blends. Because the domains in blend 1.5-1.5 could not be easily defined for $\varphi_H > 0.4$, the transition to a two-phase system was not determined for this blend. The nonuniform phase and macrophase transitions in the cylinder-forming blends occurred at φ_H values similar to the transitions in lamellae-forming block copolymer blends.[34,35]

The nonuniform phase found in this work had a number of similarities to the microemulsion phase reported in previous studies of lamellae-forming bulk and thin film ternary polymer blends. First, for the dry brush blends the nonuniform phase occurred at approximately the same value of φ_H (~0.6) as previously observed in thin film ternary blends of PS-*b*-PMMA/PS/PMMA.[34,35] Second, the lack of higher ordered peaks in the FFT spectra of the nonuniform phase mirrored the lack of higher ordered peaks in FFT spectra for microemulsions in thin films[34,35] and in SANS[21,22,57] and small-angle X-ray scattering[20] spectra of microemulsions in bulk samples. Finally, the SEM images of the nonuniform phase in this work were similar to the SEM[34,35] and transmission electron microscopy[21,22] images of microemulsions made from lamellae-forming ternary blends in that there was a wide range of domain sizes present in the images.

Wet Brush versus Dry Brush Systems. In all of the results, there was a marked difference between the 1.5-1.5 blend and the other blends. The reason for this was that the 1.5-1.5 blend contained homopolymers with M_n values much lower than the corresponding blocks of the PS-*b*-PMMA.[53] Dai et al. reported that when the homopolymer M_n in a homopolymer−block copolymer blend is much less than the M_n of the corresponding block of the copolymer, the homopolymer molecules can strongly penetrate the corresponding block, resulting in the blend forming a "wet" brush system.[58] The interpenetration of the block copolymer and the homopolymer changes the interfacial area per chain at the domain−domain interface[17,30] and possibly screens some of the interaction between blocks of the block copolymers. Because of these effects, the addition of the low M_n homopolymers in our experiments tended to shrink the block copolymer domains.

Our results with the 1.5-1.5 blend are consistent with previous research, which demonstrated that a blend of block copolymer and low M_n homopolymer can have domains that are smaller than the domains of the pure block copolymer. Quan et al. showed that the addition of low M_n polybutadiene to a poly(styrene-*b*-butadiene-*b*-styrene) A−B−A triblock copolymer decreased the size of the lamellar domains in the bulk.[59] Mykhaylyk et al. demonstrated a similar decrease in domain size of cylinders in ternary blends of poly(styrene-*b*-isoprene-*b*-styrene) A−B−A triblock copolymer, polystyrene, and polyisoprene, both in the bulk and in thin films.[32] Winey et al. showed a decrease in lamellar spacing using bulk samples of binary blends of poly(styrene-*b*-isoprene) A−B diblock copolymers with polystyrene homopolymers.[17] To the best of our knowledge, no reports have been published on the size of domains of

ternary blends of low molecular weight homopolymers with diblock copolymers in thin films, nor has any there been an investigation of these thin film blends at higher φ_H.

In contrast to blend 1.5-1.5, the other blends in this study all contained homopolymers with M_ns near the M_n of the corresponding blocks of the block copolymer. The higher M_n homopolymers in these blends are less likely to mix uniformly throughout a domain of the corresponding blocks of the block copolymer than the lower M_n homopolymers and instead tend to locate more in the center of the domain.[17,18,60,61] Because the homopolymer segregates to the center of the domain and has low interpenetration with the corresponding blocks of the block copolymer, these blends were considered to be in the "dry" brush regime. These homopolymers tend to swell the domains without significantly changing the area per chain at the domain−domain interface.

Conclusion

Our study demonstrates that the dimensions of the cylindrical morphology of a ternary blend can be increased up to 150% of the original dimensions of the pure block copolymer while retaining a high degree of uniformity. In the dry brush regime, ternary blends were useful for controlling the domain dimensions through the selection of the appropriate φ_H. Because the PS:PMMA ratio was held constant at 70:30, both D and d scaled in the same manner with φ_H, but it is reasonable to expect that varying the homopolymer ratio could lead to independent control of D and d. The best dimensional uniformity for the larger domains was obtained by using a lower M_n homopolymer within the dry brush regime. This work has also shown that small quantities of low M_n homopolymer can enhance the quality and uniformity of the cylindrical structures over a wide variety of film thicknesses. Taken together, these results might offer technological benefits in terms of the selection and control of domain size in the implementation of microphase-separated systems in lithographic and template-forming applications. In addition to the technological significance of the blends, the difference in the ordering and dimensional scaling behavior of the wet brush and dry brush blends elucidates fundamental aspects of the physics of block copolymer−homopolymer blends.

Acknowledgment. The authors thank G. S. W. Craig for help preparing the manuscript, Y.-H. La for synthesizing the brush polymer, and C.-C. Liu and Y.-H. Ting for the Si etching. Portions of this work were performed at the Center for Nanotechnology and the Synchrotron Radiation Center at the University of Wisconsin (National Science Foundation Grant DMR-0537588). This research was funded by the Global Research Collaboration (Grants 2005-OCH-985 and 2008-OCH-164) and the National Science Foundation Nanoscale Science and Engineering Center at the University of Wisconsin—Madison (Grant DMR0425880).

Supporting Information Available: Images of Si structures etched from the block copolymer template shown in Figure 1 (left). This material is available free of charge via the Internet at http://pubs.acs.org.

References and Notes

(1) Cheng, J. Y.; Ross, C. A.; Smith, H. I.; Thomas, E. L. *Adv. Mater.* **2006**, *18*, 2505.
(2) Olson, D. A.; Chen, L.; Hillmyer, M. A. *Chem. Mater.* **2008**, *20*, 869.
(3) Ruiz, R.; Kang, H.; Detcheverry, F. A.; Dobisz, E.; Kercher, D. S.; Albrecht, T. R.; de Pablo, J. J.; Nealey, P. F. *Science* **2008**, *321*, 936.
(4) Bita, I.; Yang, J. K. W.; Jung, Y. S.; Ross, C. A.; Thomas, E. L.; Berggren, K. K. *Science* **2008**, *321*, 939.
(5) Stoykovich, M. P.; Nealey, P. F. *Mater. Today* **2006**, *9*, 20.
(6) Stoykovich, M. P.; Kang, H.; Daoulas, K. C.; Liu, G.; Liu, C. C.; de Pablo, J. J.; Mueller, M.; Nealey, P. F. *ACS Nano* **2007**, *1*, 168.
(7) Xiao, S. G.; Yang, X. M. *J. Vac. Sci. Technol., B* **2007**, *25*, 1953.
(8) La, Y. H.; Stoykovich, M. P.; Park, S. M.; Nealey, P. F. *Chem. Mater.* **2007**, *19*, 4538.
(9) Nie, Z. H.; Kumacheva, E. *Nat. Mater.* **2008**, *7*, 277.
(10) Bates, F. S.; Fredrickson, G. H. *Annu. Rev. Phys. Chem.* **1990**, *41*, 525.
(11) Edwards, E. W.; Stoykovich, M. P.; Nealey, P. F.; Solak, H. H. *J. Vac. Sci. Technol., B* **2006**, *24*, 340.
(12) Jeong, U. Y.; Kim, H. C.; Rodriguez, R. L.; Tsai, I. Y.; Stafford, C. M.; Kim, J. K.; Hawker, C. J.; Russell, T. P. *Adv. Mater.* **2002**, *14*, 274.
(13) Jeong, U. Y.; Ryu, D. Y.; Kim, J. K.; Kim, D. H.; Wu, X. D.; Russell, T. P. *Macromolecules* **2003**, *36*, 10126.
(14) Torikai, N.; Takabayashi, N.; Noda, I.; Koizumi, S.; Morii, Y.; Matsushita, Y. *Macromolecules* **1997**, *30*, 5698.
(15) Orso, K. A.; Green, P. F. *Macromolecules* **1999**, *32*, 1087.
(16) Peng, J.; Gao, X.; Wei, Y. H.; Wang, H. F.; Li, B. Y.; Han, Y. C. *J. Chem. Phys.* **2005**, *122*, 114706.
(17) Winey, K. I.; Thomas, E. L.; Fetters, L. J. *Macromolecules* **1991**, *24*, 6182.
(18) Jeong, U.; Ryu, D. Y.; Kho, D. H.; Lee, D. H.; Kim, J. K.; Russell, T. P. *Macromolecules* **2003**, *36*, 3626.
(19) Hashimoto, T.; Tanaka, H.; Hasegawa, H. *Macromolecules* **1990**, *23*, 4378.
(20) Corvazier, L.; Messe, L.; Salou, C. L. O.; Young, R. N.; Fairclough, J. P. A.; Ryan, A. J. *J. Mater. Chem.* **2001**, *11*, 2864.
(21) Bates, F. S.; Maurer, W. W.; Lipic, P. M.; Hillmyer, M. A.; Almdal, K.; Mortensen, K.; Fredrickson, G. H.; Lodge, T. P. *Phys. Rev. Lett.* **1997**, *79*, 849.
(22) Hillmyer, M. A.; Maurer, W. W.; Lodge, T. P.; Bates, F. S.; Almdal, K. *J. Phys. Chem. B* **1999**, *103*, 4814.
(23) Duchs, D.; Schmid, F. *J. Chem. Phys.* **2004**, *121*, 2798.
(24) Pipich, V.; Schwahn, D.; Willner, L. *Appl. Phys. A* **2002**, *74*, S345.
(25) Duchs, D.; Ganesan, V.; Fredrickson, G. H.; Schmid, F. *Macromolecules* **2003**, *36*, 9237.
(26) Floudas, G.; Hadjichristidis, N.; Stamm, M.; Likhtman, A. E.; Semenov, A. N. *J. Chem. Phys.* **1997**, *106*, 3318.
(27) Kang, C. K.; Zin, W. C. *Macromolecules* **1992**, *25*, 3039.
(28) Kielhorn, L.; Muthukumar, M. *J. Chem. Phys.* **1997**, *107*, 5588.
(29) Likhtman, A. E.; Semenov, A. N. *Macromolecules* **1997**, *30*, 7273.
(30) Matsen, M. W. *Macromolecules* **1995**, *28*, 5765.
(31) Morkved, T. L.; Chapman, B. R.; Bates, F. S.; Lodge, T. P.; Stepanek, P.; Almdal, K. *Faraday Discuss.* **1999**, *112*, 335.
(32) Mykhaylyk, T. A.; Mykhaylyk, O. O.; Collins, S.; Hamley, I. W. *Macromolecules* **2004**, *37*, 3369.
(33) Vaidya, N. Y.; Han, C. D.; Kim, D.; Sakamoto, N.; Hashimoto, T. *Macromolecules* **2001**, *34*, 222.
(34) Liu, G.; Stoykovich, M. P.; Ji, S.; Stuen, K. O.; Craig, G. S. W.; Nealey, P. F. *Macromolecules* **2009**, *42*, 3063.
(35) Stoykovich, M. P.; Edwards, E. W.; Solak, H. H.; Nealey, P. F. *Phys. Rev. Lett.* **2006**, *97*, 147802.
(36) Zhao, J. C.; Jiang, S. C.; Ji, X. G.; An, L. J.; Jiang, B. Z. *J. Polym. Sci., Part B: Polym. Phys.* **2004**, *42*, 3496.
(37) Benoit, D.; Chaplinski, V.; Braslau, R.; Hawker, C. J. *J. Am. Chem. Soc.* **1999**, *121*, 3904.
(38) Mansky, P.; Liu, Y.; Huang, E.; Russell, T. P.; Hawker, C. *Science* **1997**, *275*, 1458.
(39) Edwards, E. W.; Montague, M. F.; Solak, H. H.; Hawker, C. J.; Nealey, P. F. *Adv. Mater.* **2004**, *16*, 1315.
(40) Russell, T. P.; Hjelm, R. P.; Seeger, P. A. *Macromolecules* **1990**, *23*, 890.
(41) Ruiz, R.; Sandstrom, R. L.; Black, C. T. *Adv. Mater.* **2007**, *19*, 587.
(42) Segalman, R. A.; Hexemer, A.; Hayward, R. C.; Kramer, E. J. *Macromolecules* **2003**, *36*, 3272.
(43) Park, S. M.; Craig, G. S. W.; Liu, C. C.; La, Y. H.; Ferrier, N. J.; Nealey, P. F. *Macromolecules* **2008**, *41*, 9118.
(44) Park, S. M.; Craig, G. S. W.; La, Y. H.; Solak, H. H.; Nealey, P. F. *Macromolecules* **2007**, *40*, 5084.
(45) Guarini, K. W.; Black, C. T.; Yeuing, S. H. I. *Adv. Mater.* **2002**, *14*, 1290.
(46) Kitano, H.; Akasaka, S.; Inoue, T.; Chen, F.; Takenaka, M.; Hasegawa, H.; Yoshida, H.; Nagano, H. *Langmuir* **2007**, *23*, 6404.
(47) Son, J. G.; Bulliard, X.; Kang, H. M.; Nealey, P. E.; Char, K. *Adv. Mater.* **2008**, *20*, 3643.
(48) Broseta, D.; Fredrickson, G. H. *J. Chem. Phys.* **1990**, *93*, 2927.

(49) Hornreich, R. M.; Luban, M.; Shtrikman, S. *Phys. Lett. A* **1975**, *55*, 269.
(50) Janert, P. K.; Schick, M. *Macromolecules* **1997**, *30*, 3916.
(51) Kaeble, D. H. *Physical Chemistry of Adhesion*; Wiley: New York, 1971; p 499.
(52) Komura, S. *J. Phys.: Condens. Matter* **2007**, *19*, 463101.
(53) Komura, S.; Kodama, H.; Tamura, K. *J. Chem. Phys.* **2002**, *117*, 9903.
(54) Muller, M.; Schick, M. *J. Chem. Phys.* **1996**, *105*, 8885.
(55) Thompson, R. B.; Matsen, M. W. *Phys. Rev. Lett.* **2000**, *85*, 670.
(56) Schubert, K. V.; Strey, R.; Kline, S. R.; Kaler, E. W. *J. Chem. Phys.* **1994**, *101*, 5343.
(57) Morkved, T. L.; Stepanek, P.; Krishnan, K.; Bates, F. S.; Lodge, T. P. *J. Chem. Phys.* **2001**, *114*, 7247.
(58) Dai, K. H.; Kramer, E. J.; Shull, K. R. *Macromolecules* **1992**, *25*, 220.
(59) Quan, X.; Gancarz, I.; Koberstein, J. T.; Wignall, G. D. *Macromolecules* **1987**, *20*, 1431.
(60) Mayes, A. M.; Russell, T. P.; Satija, S. K.; Majkrzak, C. F. *Macromolecules* **1992**, *25*, 6523.
(61) Leibler, L. *Makromol. Chem., Macromol. Symp.* **1988**, *16*, 1.